

Investigating River-Surge Interaction in Idealised Estuaries

Author(s): John Maskell, Kevin Horsburgh, Matthew Lewis and Paul Bates

Source: *Journal of Coastal Research*, Vol. 30, No. 2 (March 2014), pp. 248-259

Published by: Coastal Education & Research Foundation, Inc.

Stable URL: <https://www.jstor.org/stable/43290051>

Accessed: 17-06-2019 12:44 UTC

REFERENCES

Linked references are available on JSTOR for this article:

https://www.jstor.org/stable/43290051?seq=1&cid=pdf-reference#references_tab_contents

You may need to log in to JSTOR to access the linked references.

JSTOR is a not-for-profit service that helps scholars, researchers, and students discover, use, and build upon a wide range of content in a trusted digital archive. We use information technology and tools to increase productivity and facilitate new forms of scholarship. For more information about JSTOR, please contact support@jstor.org.

Your use of the JSTOR archive indicates your acceptance of the Terms & Conditions of Use, available at

<https://about.jstor.org/terms>



JSTOR

Coastal Education & Research Foundation, Inc. is collaborating with JSTOR to digitize, preserve and extend access to *Journal of Coastal Research*

Investigating River–Surge Interaction in Idealised Estuaries

John Maskell^{†*}, Kevin Horsburgh[†], Matthew Lewis[†], and Paul Bates[‡]

[†]National Oceanography Centre
Liverpool, Merseyside L3 5DA, U.K.

[‡]Bristol University
Clifton, Bristol BS8 1SS, U.K.



www.cerf-jcr.org

ABSTRACT



www.JCRonline.org

Maskell, J.; Horsburgh, K.; Lewis, M., and Bates, P., 2014. Investigating river–surge interaction in idealised estuaries. *Journal of Coastal Research*, 30(2), 248–259. Coconut Creek (Florida), ISSN 0749-0208.

A finite volume model (FVCOM) was used to investigate the combined influence of storm surge and river flow on floodplain inundation on the basis of idealized estuary test cases. The combined influence of storm surge and river discharge typical of extremes in estuary systems in Britain (up to 2 m and $1500 \text{ m}^3 \text{ s}^{-1}$) was found to induce interactions that lead to increases in the nontidal residual elevation of up to 0.35 m. However, the extent of the inundation was found to be mainly controlled by the surge elevation. Exceeding the threshold of the up-estuary channel capacity was found to cause a nonlinear increase in the area of the nontidal inundation for any given peak river discharge, after which the rate of increase in inundation area as the surge height increases declines and is determined by the slope of the floodplain. This threshold is determined by the surge elevation with exception of the highest peak river discharges, where the surge elevation threshold is lowered. It was also found that the extent of the interactions and inundation were highly dependent on the geometry of the estuary and the timing of the surge with respect to peak river discharge, in particular the slope of the floodplain and at such times where the river discharge was similar in magnitude to that of the surge and the tide. After calibration an idealized estuary based in the LISFLOOD-FP code, using a simplified form of the two-dimensional (2D) shallow-water equations, was found to simulate the area of maximum inundation to a similar extent as the FVCOM model (based on the full 2D shallow-water equations) with a much reduced computation time. This paper highlights the potential advantages that simplified 2D inundation models may have for simulating estuarine flooding due to combined surge and river discharge, where surge–river interaction due to momentum exchange is insignificant in determining the flood extent and simplified equations capture the dominant hydrological drivers of coastal inundation.

ADDITIONAL INDEX WORDS: *Estuary, flooding, storm surge, modelling.*

INTRODUCTION

In coastal areas, particularly in regions developed on estuaries, extreme river flow can combine with storm surges to present a combined flooding hazard. This combined risk is likely to be more prominent in estuaries where fluvial freshwater input comes from catchments in hilly regions where the dependence of extreme river discharge and sea-level elevation can be most statistically significant (Svensson and Jones, 2004). For example, this study is applicable to U.K. estuaries such as the Eden Estuary in NW England. The region is affected by storm surges with a 50-year return-period sea level of 5.7 m at nearby Workington. The upper catchment of the River Eden is dominated by mountainous terrain consisting of hard volcanic rocks and thin soils so that runoff during heavy rain is very rapid. The short lag time in the hydrograph means that high sea levels could combine with high river levels driven by the same weather system.

The risk associated with these combined coastal hazards could increase due to climate change if there was an increase in the frequency of extreme weather events. Recent research on climate projections described in the U.K. Climate Projections 2009 (Lowe *et al.*, 2009) shows that the statistical significance of any trends in enhanced storminess and storm-surge

generation is small. However, the global (IPCC, 2007) and local (Woodworth *et al.*, 2009) rise in mean sea level will increase the magnitude of extreme sea levels and surges will act on a higher coastal sea level and therefore increase the risk to coastal property and infrastructure. This may be associated with an increase in precipitation during extreme storm events, which will have a large impact on river flooding. Future increase in sea level has a wide range of socioeconomic impacts, with some regions being more vulnerable, particularly in low-lying coastal regions where both surges and river floods will have an increased impact (see Nicholls, 2002). The predicted trend of an increased frequency of damaging events means that in some locations any current levels of protection are likely to be insufficient in the future. Therefore, the need for accurate operational forecasting of storm events will increase, with the focus shifting to changes in the extreme “tail end” of the distribution of storm events.

Ideally an operational model that integrates storm surge, wave, and fluvial forecasting with inundation and simulates their combined influence would be most effective for planning with respect to floodplain development, evacuation, and implementation of flood defences. It is important to understand whether extreme river discharge can interact in a nonlinear manner with extreme sea levels driven by the same weather system. Although hydraulic control is known to be important in controlling the discharge in two-layer flows (*e.g.*, Armi, 1986), it is not known how relevant it is to the flow of floodwaters combined with high tidal flow in a well-mixed or partially

DOI: 10.2112/JCOASTRES-D-12-00221.1 received 31 October 2012; accepted in revision 2 April 2013; corrected proofs received 11 July 2013.

Published Pre-print online 8 August 2013.

*Corresponding author: maskers@hotmail.co.uk
© Coastal Education & Research Foundation 2014

mixed estuary or the spatial extent of the interaction and its effect on the resultant inundation.

Modelling inundation in coastal regions is dependent on simulating three types of flow transition: the flow between the coast and dry land, the essentially one-dimensional (1D) flow in channels to two-dimensional (2D) flow over land, and subcritical to supercritical flow (Battjes and Gerritsen, 2002). The governing equations of the motion of water masses are expressed by the conservation of momentum, mass, and energy in a unit volume. This cannot always be guaranteed when solving the equations numerically and most modelling solutions strive to simulate the dominant physical processes whilst remaining numerically stable. Predicting coastal sea-level elevations due to tide, surges, and waves for operational purposes is typically carried out using 2D models (*e.g.*, Flather, 2000). Most of these models can accurately predict coastal sea-level elevations where the most significant errors arise from the accuracy of the forcing meteorology (*e.g.*, Flowerdew *et al.*, 2010) or the resolution of the model grid (*e.g.*, Jones and Davies, 2005). Development of finite element solutions of the shallow-water equations, which give stable solutions by modifying the governing equations (Lynch and Gray, 1979), meant that unstructured grids of variable resolution could be applied to coastal models. High-resolution grids in shallow-water coastal regions may permit tide and surge elevations and their associated currents to be simulated more accurately (*e.g.*, Jones and Davies, 2008; Westerink, Luettich, and Muccino, 1994). Finite volume models (*e.g.*, FVCOM) offer the geometric flexibility of the finite element method with the simple, discrete computational efficiency of the finite difference method where the governing equations are solved in their integral form so that laws of conservation are more readily adhered to (Chen, Liu, and Beardsley, 2003). However, solving the full 2D shallow-water equations remains relatively computationally expensive, particularly when resolving topographic features of 50 m or less, which is essential for simulating flooding in urbanised coastal areas (Bates *et al.*, 2005). In addition, 2D models for coastal and estuarine flow are not well suited to flood modelling on floodplains where initially dry land is inundated and supercritical flow conditions can occur (McCowan, Rasmussen, and Berg, 2001).

In a risk-based framework a large number of surge, tide, and river flow conditions need to be simulated in a computationally efficient manner. Therefore, there is a need to develop simplified 2D models for coastal flooding that are more computationally efficient whilst still simulating the dominant hydrological drivers of coastal flooding (Bates *et al.*, 2005). For example, the LISFLOOD-FP model originally developed by Bates and De Roo (2000) can simulate 1D and 2D flows in terms of the continuity and momentum equations on a raster grid where 1D channel flow is simply a response of the free surface slope and flow between cells on the floodplain is a function of the free surface height difference between adjacent cells (Bates *et al.*, 2005). Models such as these have been developed by taking advantage of increased availability of high-accuracy, fine spatial resolution topographic data from remote-sensing techniques such as airborne laser altimetry and light detection and ranging (*e.g.*, Marks and Bates, 2000). For fluvial flooding (*e.g.*, Horritt and Bates, 2002) such models have been shown to

perform as well as full 2D models at predicting maximum inundation during dynamic events. For inundation modelling these are typically based on cell-storage models (see Bates and De Roo [2000] for a summary of the various cell-storage approaches in the literature). These are often based on simplified versions of the Saint-Venant equations obtained by eliminating local acceleration, convective acceleration, and pressure terms in the momentum equation so that the friction and gravity forces balance (Bates and De Roo, 2000). Flow between two cells is simply a function of the difference in free surface height between them. Channel flow can be treated using a 1D approach with a 2D approach applied to flood propagation on the floodplain after bankfull in the channel. The simplified nature of the equations makes cell-storage models extremely computationally efficient so that thousands of simulations can be carried out using different forcings in a probabilistic framework (*e.g.*, on the basis of stochastic rainfall models) and ensemble simulations can be readily carried out to fully sample the range of uncertainty using a Monte Carlo approach (Bates *et al.*, 2005). They can also take advantage of high-resolution topography using fine grid resolution (Horritt and Bates, 2001).

Although it is assumed that this simplified approach captures most of the dominant processes in inundation despite some missing physics, they are based on some assumptions and often require certain modifications in the numerical scheme to make them applicable. The diffusion wave equations used for channel flow assumes the channel to be wide and shallow so the wetted perimeter is approximated by the channel width. Using the coupled 1D/2D approach assumes the flow is gradually varying so that there is only mass transfer between the channel and the floodplain with no channel floodplain momentum transfer and does not include supercritical effects (Prestininzi *et al.*, 2011). In the 1D channel backwater effects are neglected as well as the development of shock waves in areas of flow convergence (Bates and De Roo, 2000). Describing the channel flow using a kinematic wave approximation requires the downstream slope to be negative and the 2D floodplain flow does not fully represent diffusive wave propagation due to decoupling of the *x*- and *y*-components of the flow (Bates *et al.*, 2005). For use in coastal flood inundation the simplified hydrodynamics will usually break down in deep water.

The models are often more sensitive to channel, rather than floodplain, friction so that stringent calibration is often necessary. However, optimal parameter sets may differ for different flood events, decreasing the model's value in a predictive sense (Horritt and Bates, 2002). A flow limiter is often required to prevent too much water leaving a cell during a time step. This can also be achieved by using an adaptive time step so that the minimum time step required for updating the depth is implemented at each time step (Bates, Horritt, and Fewtrell, 2010). These issues and the need for strict control arise from the lack of mass and inertia where inertia would act to reduce the intercell fluxes at each time step. This can be reduced by including acceleration terms in the equations so that water has mass, which prevents too much water leaving a cell during a time step and rapid flow reversal. Representing shallow-water wave propagation in this manner permits longer time steps and means the solutions are less dependent on grid

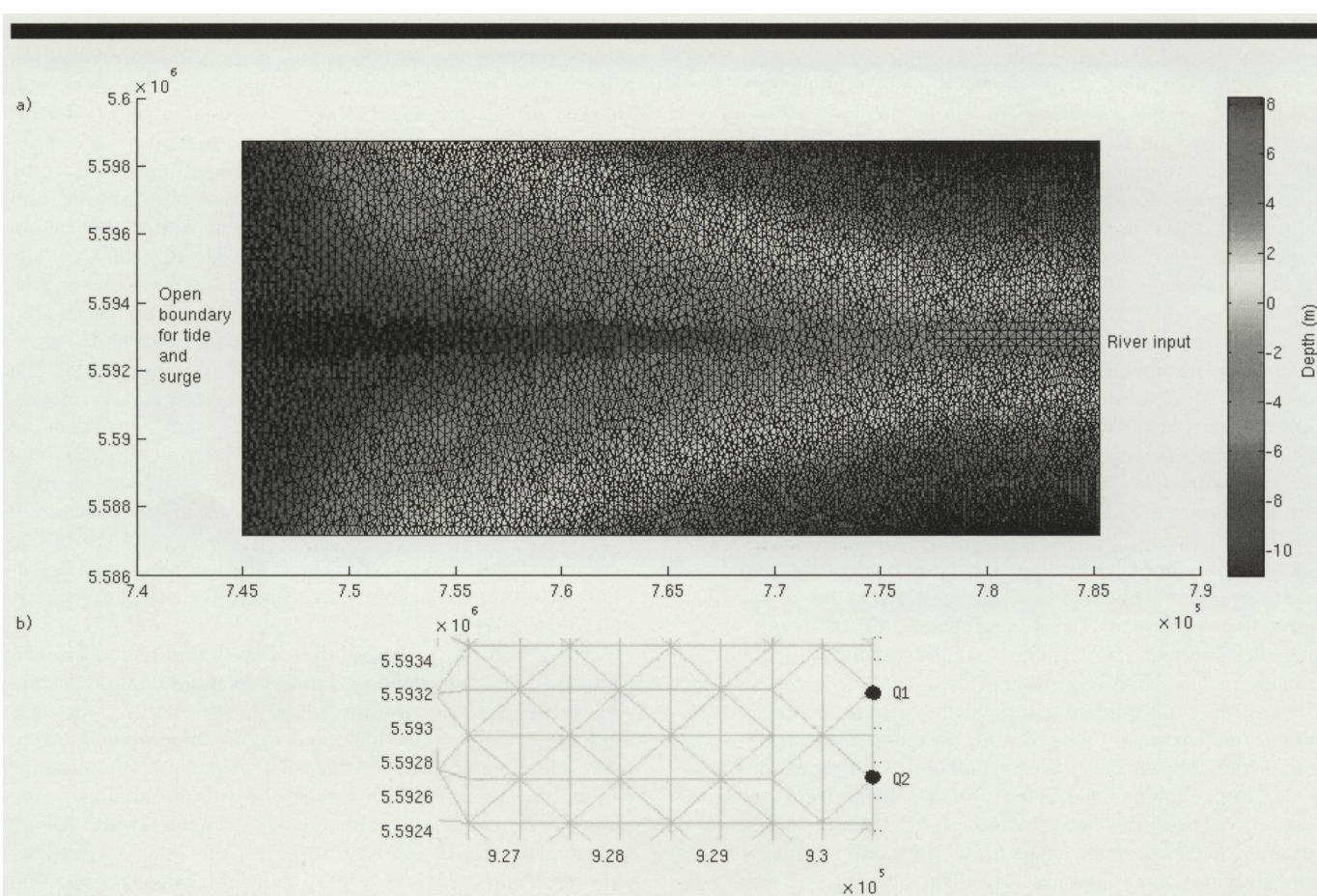


Figure 1. (a) Idealised estuary (IE1) bathymetry and finite element grid. (b) Close-up of river subgrid (IE2) with two river discharge points at boundary nodes (Q1 and Q2). (Color for this figure is available in the online version of this paper.)

size. However, instabilities can occur at low friction values typical of urban areas (Bates, Horritt, and Fewtrell, 2010).

Despite these limitations these raster-based codes have been shown to perform as well as full 2D finite element models (*e.g.*, Horritt and Bates, 2001). In many cases for inundation the accuracy of the topography may be more important than accuracy of the physics in the model. In coupled models, despite limitations in the simulated channel flow, as long as bankfull discharge is approximately correct the flood extent may be simulated accurately as the flood front is far-field to the channel and any significant errors are damped out (Horritt and Bates, 2001). However, in some instances such as during the combination of high river discharge and high sea levels due to tide and storm surge in estuaries, some of the missing physics such as momentum exchange may become important in determining the spatial extent of the inundation.

In this paper surge and river interaction is investigated using idealized estuaries focusing on the effect of the estuary geometry and the magnitude of the surge *vs.* the river discharge. Idealized estuaries are useful tools for studying estuarine dynamics where the geometry of a typical estuary can be reasonably approximated and the most important drivers of estuarine dynamics simulated in a computationally

efficient manner, allowing many test cases to be simulated. For example, idealized estuaries have been used to simulate lateral estuarine circulation and the implications for sediment transport and estuary morphology (Chen and Sanford, 2009), the vertical estuarine structure and salt transport (Chen and Sanford, 2009), and the flood and ebb dominance of sediment transport (Robins, 2008).

The importance of model formulation in simulating inundation due to surge and river discharge is also investigated by using FVCOM, which solves the full 2D depth- integrated shallow-water equations, and LISFLOOD-FP, which utilizes a simplified form of the governing equations.

METHODS

Surge and river interaction was investigated in idealised estuaries using the FVCOM model. Various idealised estuary model grids were built, a deep funnel-shaped estuary (IE1) (Figure 1a) and two shallower, more elongate estuaries with different intertidal bed slopes (IE2 and IE3). Funnel-shaped estuaries were used to capture the transition between an open macrotidal estuary and the region where many estuaries narrow, at the upper extent of tidal influence in the river channel.

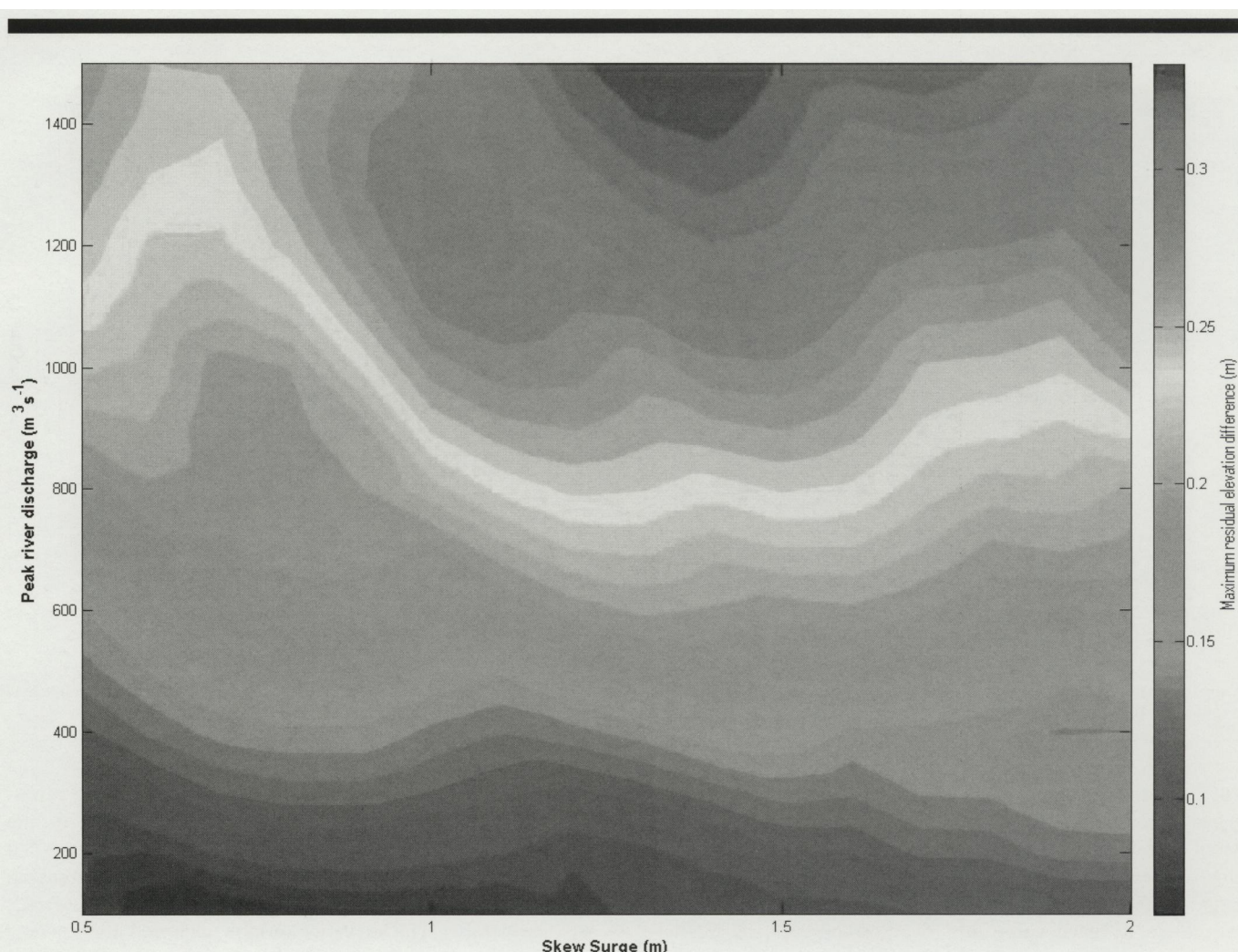


Figure 2. Maximum difference in elevation due to river–surge interaction for combined skew surge (0.5–2 m) and river discharge (100–1500 $\text{m}^3 \text{s}^{-1}$) in IE1. (Color for this figure is available in the online version of this paper.)

The finite volume method permits the use of a grid with variable grid resolution (150 m to 25 m) so that large elements can be used in the deeper open entrance of the estuary and the main channel with smaller elements on the intertidal zones so that resolution at the inundation front is not lost. A river subgrid (Figure 1b) was also implemented within the main grid so that the river discharge could be split equally over two closed boundary nodes (Q1 and Q2) into equilateral triangular elements as required in FVCOM and so that resolution in the region of river discharge can be controlled and is not diminished on the unstructured grid. The slope of the estuary as you approach the open entrance is increased until the sides are perpendicular, creating a deep open entrance, removing the need to simulate shelf outside the estuary so that the tide and surge can be introduced at the entrance to the estuary. This change in shape also reflects the transition to a sharply incised channel observed in many coastal plain estuaries (*e.g.*, Chen and Sanford, 2009).

An initial tidal simulation was carried out on each model grid, forcing the model with an M_2 tide of 2 m amplitude using a 30-second time step and including the effect of Coriolis at a latitude of 54° N, comparable with the Eden Estuary. Each model was then forced with skew surge amplitudes ranging in height from 0.5 m to 2 m in steps of 0.1 m and then river discharges based on idealised sinusoidal hydrographs with peak discharges ranging from 100 $\text{m}^3 \text{s}^{-1}$ to 1500 $\text{m}^3 \text{s}^{-1}$ in steps of 100 $\text{m}^3 \text{s}^{-1}$ and a background river discharge of 50 $\text{m}^3 \text{s}^{-1}$. The river discharges chosen are applicable to river discharge in Britain (*e.g.*, the Eden). When considering estuaries in other regions of the world, higher peak flows may need to be used to fully quantify the surge–river interaction. A skew surge is the difference in elevation between the high water and the predicted tidal high water. In these experiments the surge was equivalent to an increase in the tidal amplitude with no phase shift in the tide at the open boundary input. Further simulations were then carried out with every possible combination of surge and river discharge. Interaction between the

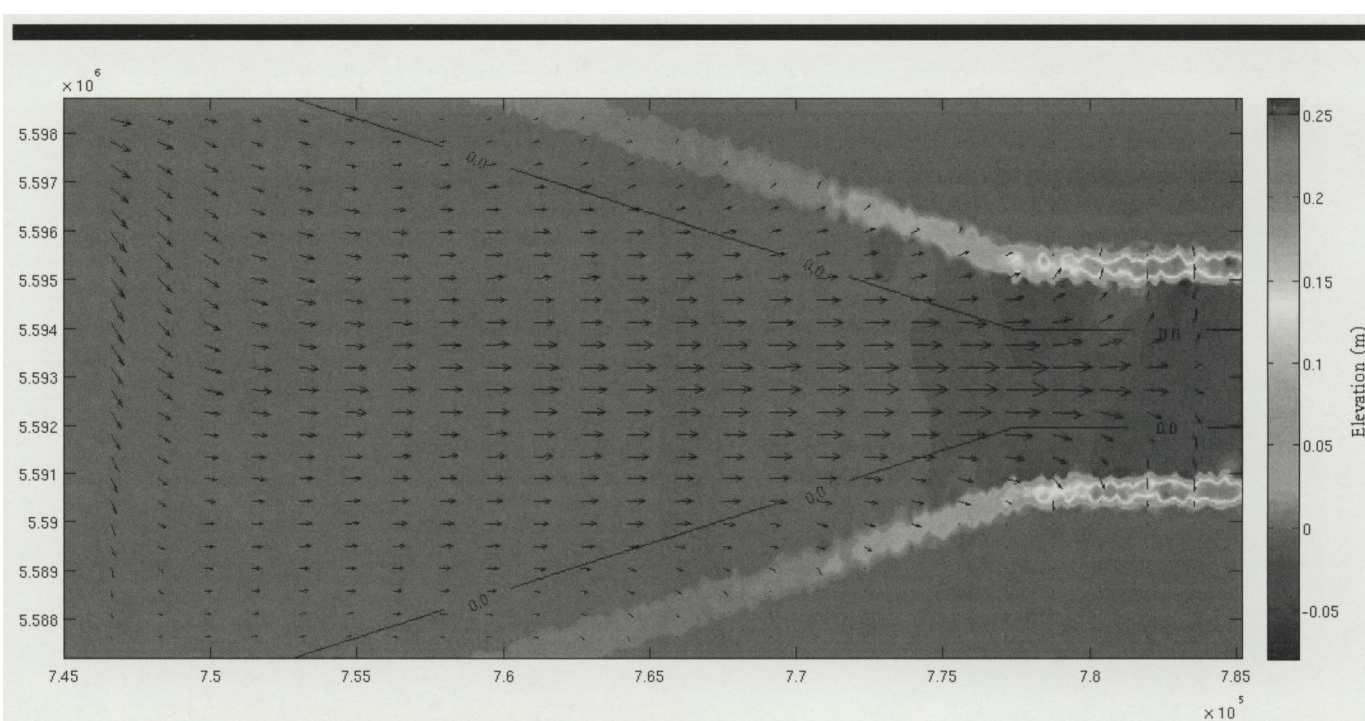


Figure 3. Region of peak interactions and current vectors in IE1 for a combined skew surge of 2 m and a river discharge of $1400 \text{ m}^3 \text{ s}^{-1}$. (Color for this figure is available in the online version of this paper.)

surge and river components in the combined solution was investigated by calculating the difference between the simulated elevations in the combined solution and the elevations due to the sum of the river and surge components simulated separately. The maximum area of inundation was also calculated for each surge and river combination. A further experiment was carried out in which the timing of the peak surge with respect to the peak river discharge was altered at hourly intervals to examine the effect on the maximum area of inundation. The model was forced with tide and surge at the open western boundary of the grid (Figure 1a) and the river discharge was included at two nodes at the eastern boundary (Figure 1a) at a river subgrid nested into the main grid along the central line of the estuary. The FVCOM model was forced for three tidal cycles or 72 hours with a 30-second time step introducing the surge on the third tidal cycle to allow the model time to “spin up” from a cold start. In this study we assumed that the estuary is macrotidal and well mixed and the effects of three-dimensional density structure are negligible compared with dominant drivers of inundation (river discharge and sea-level elevation). It also meant that a comparison could be made between the inundation simulated by FVCOM and that of a simplified 2D model (LISFLOOD-FP) that neglects these effects, which are computationally expensive to simulate especially if used in an ensemble-based approach.

A further idealized estuary (IE4) was built to compare FVCOM with LISFLOOD-FP. Whereas FVCOM solves the full 2D shallow-water equations, LISFLOOD-FP solves simplified forms of the governing equations. The formulation in LISFLOOD-FP is derived from the momentum equation of the

quasi-linearized 1D shallow-water equations. The code represents shallow-water wave propagation, as opposed to the diffusive wave propagation simulated in previous storage-cell models, which permits the use of a longer time step, decreasing the total computation time (see Bates, Horritt, and Fewtrell, 2010 for details). The advection term is neglected and the flow is defined per channel width. The acceleration term is included in the formulation, which is advantageous over previous storage-cell codes (e.g., Bates *et al.*, 2005), as the simulated flow has mass so that the code is less likely to initiate rapid flow reversals. The bathymetry and open-boundary tide and surge inputs and river discharges used were the same in both models. However, the FVCOM model was based on an unstructured irregular grid (150 m to 25 m) and the LISFLOOD-FP model was based on a regular grid comparable with the average resolution of the FVCOM grid with a constant resolution of 100 m. A combined surge and river test case that did not inundate the entire model domain was carried out, forcing both models with a skew surge of 2 m and river discharge of $600 \text{ m}^3 \text{ s}^{-1}$. Therefore, differences in the simulated flood front could be examined. The LISFLOOD-FP model consists of 4320 grid cells and took approximately 20 seconds to run on a Windows machine with a two-core Intel processor and an adaptive time step initially set at 100 seconds, whereas the FVCOM model, which consists of 6621 triangular elements, took approximately 8 minutes to run on parallel processors on a cluster in the Linux environment. The LISFLOOD-FP model was tuned to match the tide in the FVCOM model as closely as possible by altering the Manning’s coefficient of friction so that the root mean square difference (RMSD) in the time series of elevation along

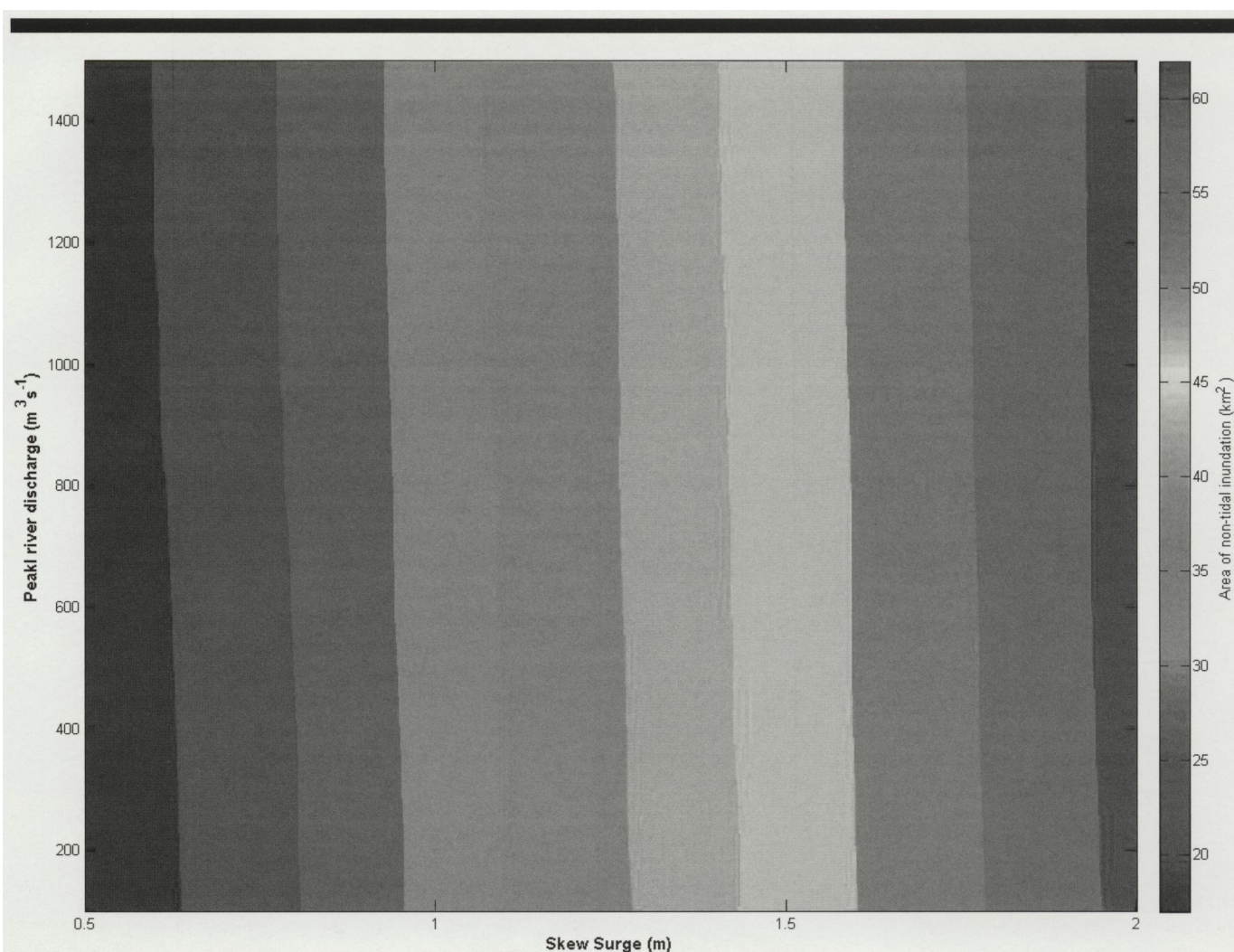


Figure 4. Area of nontidal inundation for combined skew surge (0.5–2 m) and river discharge ($100\text{--}1500\text{ m}^3\text{ s}^{-1}$) in IE1. (Color for this figure is available in the online version of this paper.)

the central channel of the estuary was reduced to a minimum. The LISFLOOD-FP model uses the Manning roughness coefficient for the frictional component within the flow approximation (see Bates *et al.*, 2005; Bates, Horritt, and Fewtrell, 2010), which is typically adjusted during model calibration (e.g., Lewis *et al.*, 2011). Therefore, a range of Manning roughness coefficients were used (0.002 to 0.02) on the basis of previous simulations of LISFLOOD-FP estuary simulations (see Bates *et al.*, 2005; Lewis *et al.*, 2011, 2012), and a value was 0.008 was found to closely simulate the FVCOM water levels. Therefore, the model was tuned in a predictive sense to examine differences in the simulated flood extent as opposed to tuning the LISFLOOD-FP model with respect to the flood extent in the FVCOM model. Time series of the elevation in various regions of the estuary and of the inundation were created and the maximum area of inundation was calculated. Plots of the spatial extent of inundation were also created so differences in simulating the flood front on both models could be visualised.

RESULTS

Figure 2 shows that in IE1 there are nonlinear interactions occurring in the combined surge and river solution so that the two components combine to produce elevations within the estuary that are higher than the linear summation of the separate river and surge components for every river and surge combination. A maximum interaction occurs for skew surges of approximately 1.4 m and peak river discharges greater than $1400\text{ m}^3\text{ s}^{-1}$, producing elevations in the estuary up to 0.35 m higher than the sum of the separate river and surge components. However, the increased elevations shown in the plot are not specific to any particular location or time of occurrence and are simply based on the maximum for each surge and river combination. Figure 3 shows where the maximum interactions are taking place and the depth-averaged current vectors at the time. It can be seen that the increased elevations occur in the region of the river discharge above the mean water level (0 m contour). Current vectors at

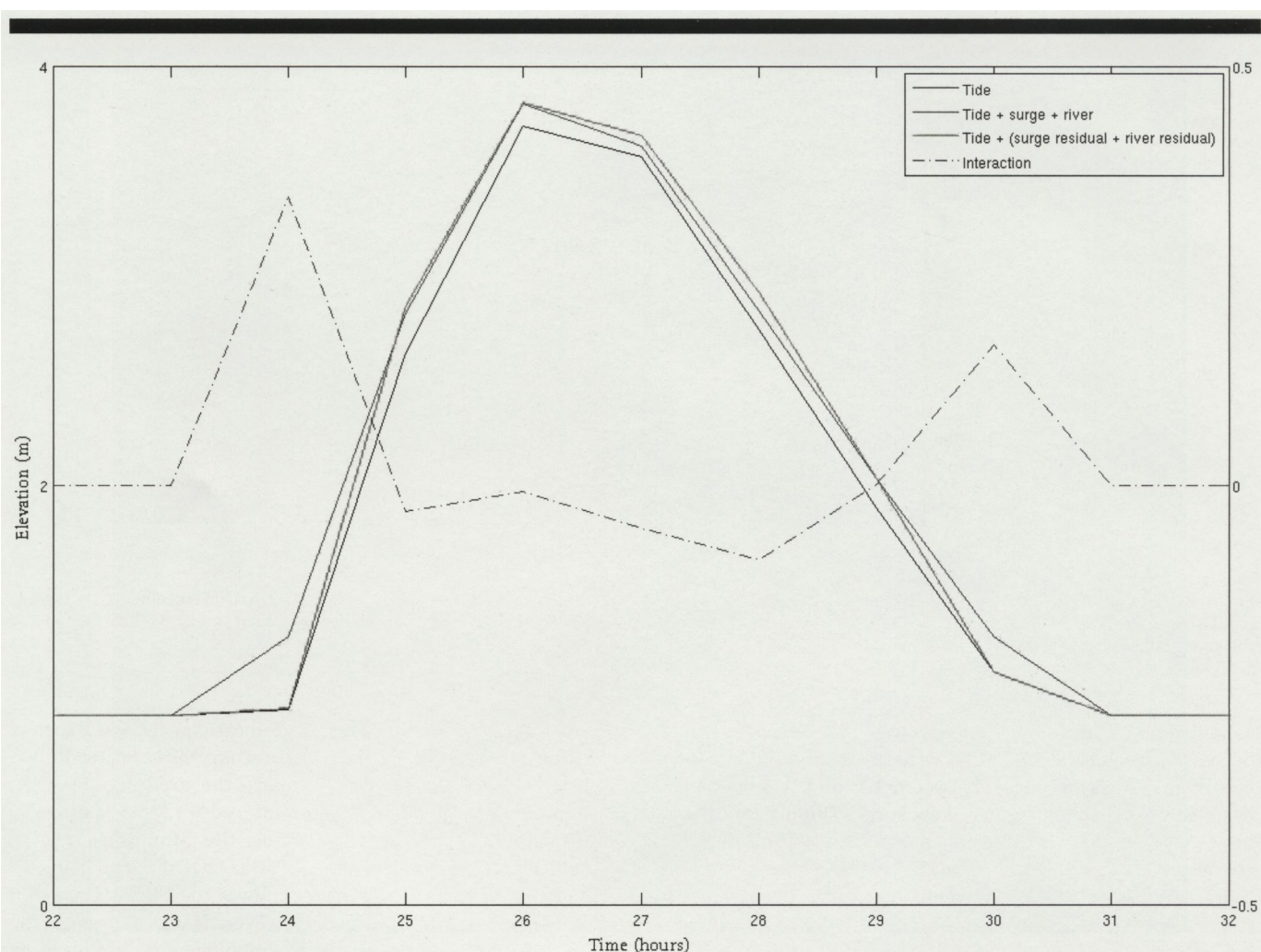


Figure 5. Time series of combined surge and tide, combined surge, tide, and river discharge, and the linear summation of tide and separate surge and river elevations including the interaction, which is the difference between the combined solution (tide, surge, and river discharge) and the linear summation of the separate (tide + surge + river discharge) solution in the region of maximum interaction in IE1. (Color for this figure is available in the online version of this paper.)

the time are in the onshore direction so that increased elevations may have implications for increased flooding of the intertidal zone. However, looking at the maximum area of nontidal inundation for each surge and river input (Figure 4), it can be seen that the increase in nontidal inundation was dominated by, and proportional to, the skew surge magnitude with no increases in the maximum area of inundation for combinations of skew surge and river discharge that induce the largest interactions. Time series of the elevations in the upper-estuary in the region of maximum interaction (Figure 5) show that the peak interactions occur at the beginning of the flood phase and at the end of the ebb phase. These interactions appear to be real increases in elevation as opposed to a phase shift of the tide and surge propagation, which would lead to a significant residual. They occur when the river discharge is similar in magnitude to the tide and surge propagation, leading to hydraulic increases in the elevation as the flow converges on the flood phase and the ebb phase is reinforced in the region of

river discharge. During peak surge the up-estuary flow is more significant than the river discharge and the river does not significantly alter the hydraulics of the flow so that the magnitude of the flood elevation is the same in the combined solution as the sum of the separate surge and river components and is mainly determined by the surge magnitude.

In the more elongate estuaries IE2 and IE3 the river discharge is very much decoupled from the peak surge elevations in the mid-estuary. In these two cases it is found that interactions between the river and surge components in terms of elevation increases are insignificant. Again, increases in the maximum area of inundation are almost linear and are mainly determined by the skew surge magnitude (Figure 6a). However, there is a threshold that causes small increases in the maximum inundation area at higher peak river discharge magnitudes where the river cannot be contained in the upper channel and flows onto the floodplain. As expected, the maximum area of inundation decreases as the intertidal

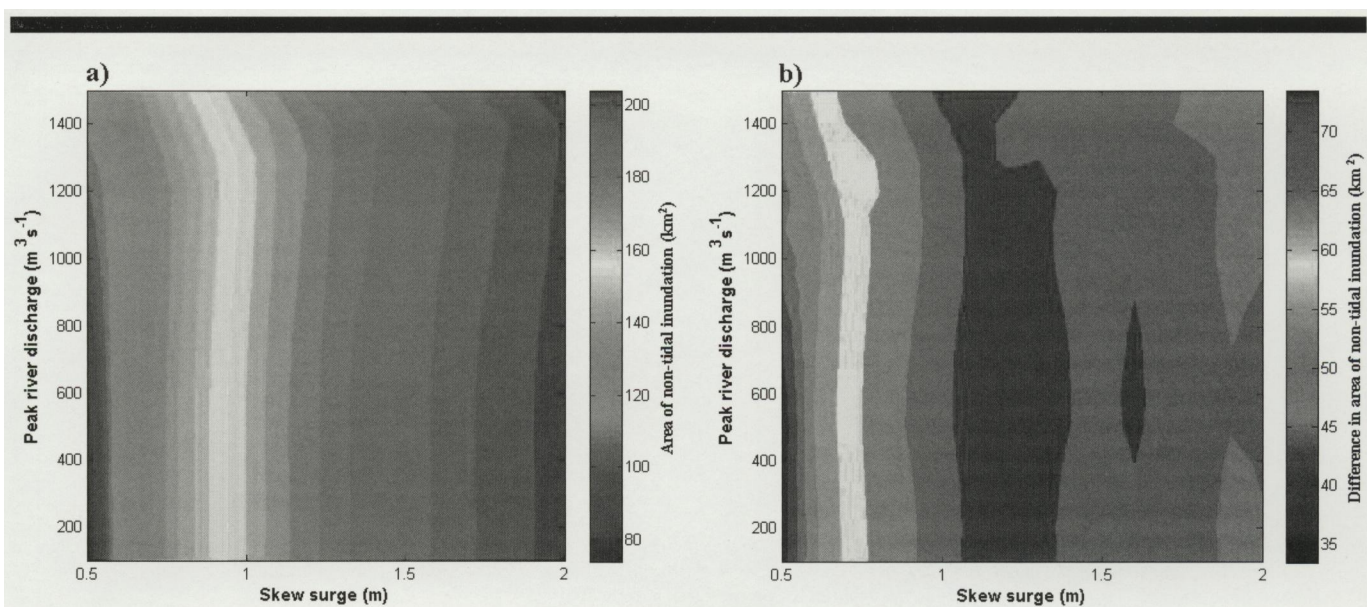


Figure 6. (a) Area of nontidal inundation for combined skew surge (0.5–2 m) and river discharge (100–1500 $\text{m}^3 \text{s}^{-1}$) in IE2. (b) Difference in area of nontidal inundation for combined skew surge (0.5–2 m) and river discharge (100–1500 $\text{m}^3 \text{s}^{-1}$) in IE2 and IE3 due to intertidal zone gradient (4×10^{-4} – 9×10^{-4}). (Color for this figure is available in the online version of this paper.)

zone/floodplain gradient increases in IE3. However, the decrease is seen to be nonlinear, with the maximum decreases occurring for skew surge between 1.1 and 1.3 m before decreasing slightly for higher skew surges (Figure 6b). It can be seen that in the more elongate estuaries the flooding due to the surge and the flooding due to the river is decoupled so that there is little interaction between the two flood components (Figure 7). The surge and the river both inundate the floodplain before any interaction can occur in the mid-estuary. The effect of altering the timing of peak river discharge with respect to the peak skew surge was investigated to examine whether the timing of up-estuary surge propagation could lead to more inundation if there is a delay in the peak river discharge. It was found that the timing of the peak river discharge with respect to the peak skew surge does alter the area of inundation. However, the area of inundation is mainly determined by the magnitude of the skew surge and the differences are insignificant compared with the total area of inundation (up to $\sim 4\%$).

In a final experiment an idealized estuary in FVCOM (IE4) was compared with an idealized estuary of identical dimensions in LISFLOOD-FP to compare the area of inundation simulated using the two different codes. After tuning the LISFLOOD-FP model by altering the Manning's friction coefficient it can be seen that LISFLOOD-FP can simulate the tide and surge almost identically to the FVCOM model in the mid-estuary (Figure 8a). However, it can be seen in the upper estuary that there is a more significant difference in the elevations simulated by both models where FVCOM simulates a slightly higher elevation during the second high water and then a lower peak high water during the time of peak skew surge (Figure 8b). Examining the inundation 6 hours before the maximum inundation, it can be seen that the flood extent simulated by LISFLOOD-FP is very similar to that of FVCOM (Figure 9a). However, the flood front simulated in FVCOM is slightly more advanced than that of LISFLOOD-FP, where more triangular elements in the FVCOM model have become

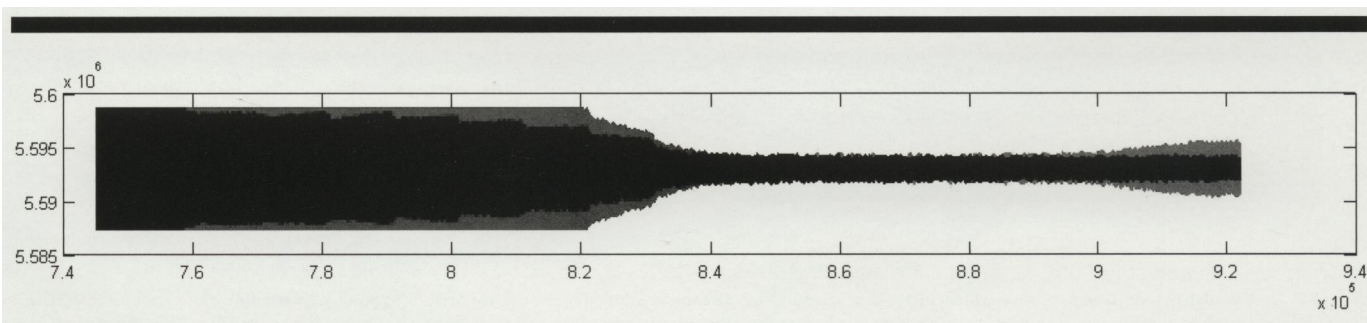


Figure 7. Dominant source of nontidal inundation due to surge (blue) and river discharge (red) in IE2. (Color for this figure is available in the online version of this paper.)

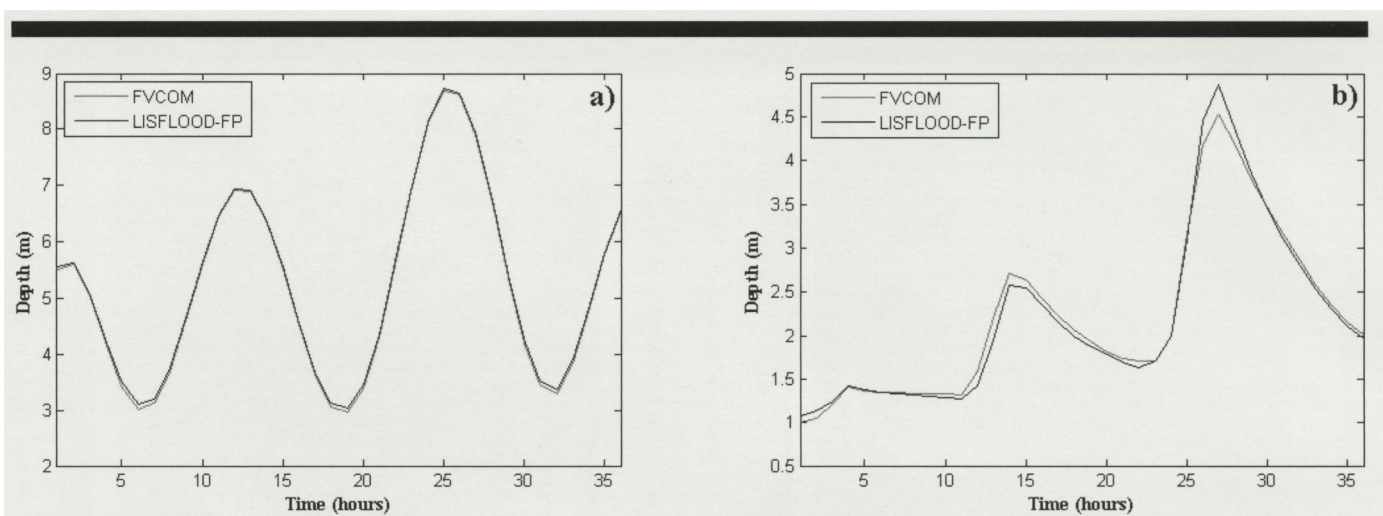


Figure 8. (a) Time series of the simulated tide, surge (2 m), and river discharge ($600 \text{ m}^3 \text{ s}^{-1}$) in the mid-estuary of an idealised estuary (IE4) based in FVCOM and LISFLOOD-FP. (b) Time series of the simulated tide, surge (2 m), and river discharge ($600 \text{ m}^3 \text{ s}^{-1}$) in the upper estuary of an idealised estuary (IE4) based in FVCOM and LISFLOOD-FP. (Color for this figure is available in the online version of this paper.)

"wet" before grid cells in the LISFLOOD-FP model. Looking at the maximum inundation simulated by both models (Figure 9b) it can be seen that the domain is almost fully inundated in both models, with a similar spatial extent of inundation. Time series of the area of inundation (Figure 10) show that LISFLOOD-FP tends to simulate a lower inundation area throughout most of the time series, with a mean difference (FVCOM – LISFLOOD-FP) of 1.44 km^2 and RMSD of 1.56 km^2 . However, it is observed

that the peak area of inundation is simulated to similar extent using both models. It appears that both models converge on a similar extent of peak inundation using the same forcing if the LISFLOOD-FP model is tuned with respect to the tide and along the channel centerline by altering the friction coefficient, where FVCOM inundates 98.2% of the domain compared with LISFLOOD-FP, which inundates 98.9% of the domain. LISFLOOD-FP inundates an area of 0.28 km^2 more than FVCOM,

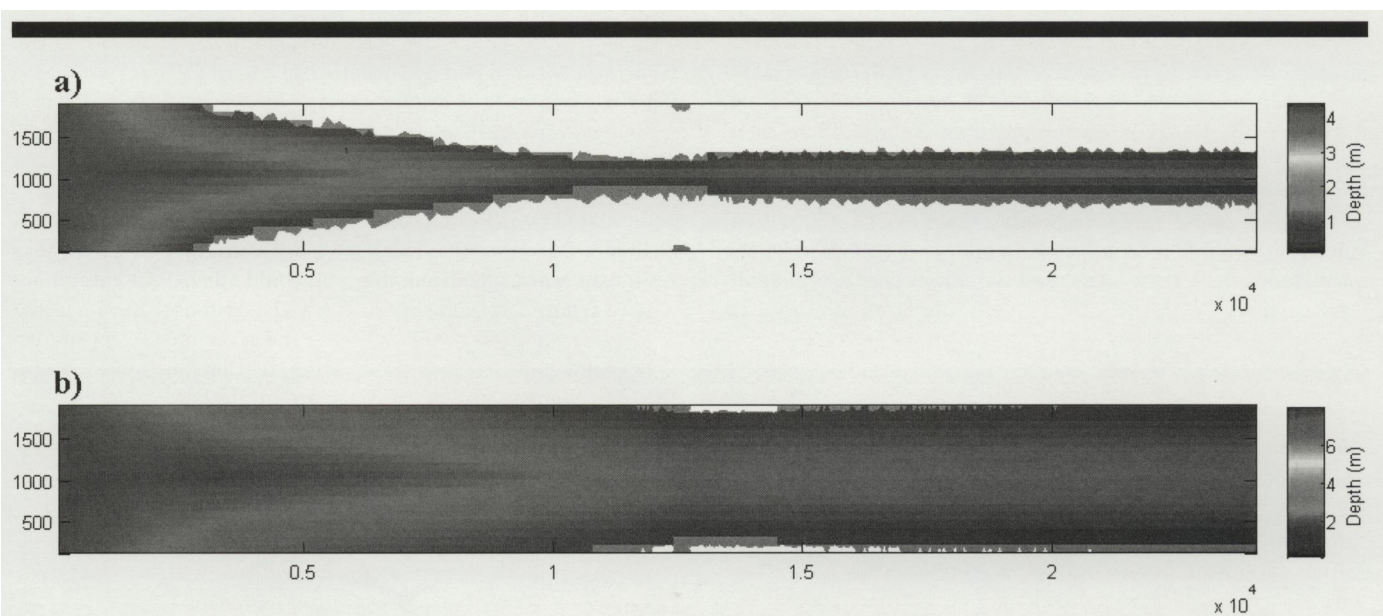


Figure 9. (a) Simulated inundation in IE4 6 h before maximum inundation due to a combined tide, surge (2 m), and river discharge ($600 \text{ m}^3 \text{ s}^{-1}$) in LISFLOOD-FP (colour plot of depth at each grid cell) and FVCOM (grey scale). (b) Simulated maximum inundation in IE4 due to a combined tide, surge (2 m), and river discharge ($600 \text{ m}^3 \text{ s}^{-1}$) in LISFLOOD-FP (colour plot of depth at each grid cell) and FVCOM (grey scale). N.B. The grey scale overlies the colour plot and highlights where the flood extent predicted by FVCOM exceeds that of LISFLOOD-FP. (Color for this figure is available in the online version of this paper.)

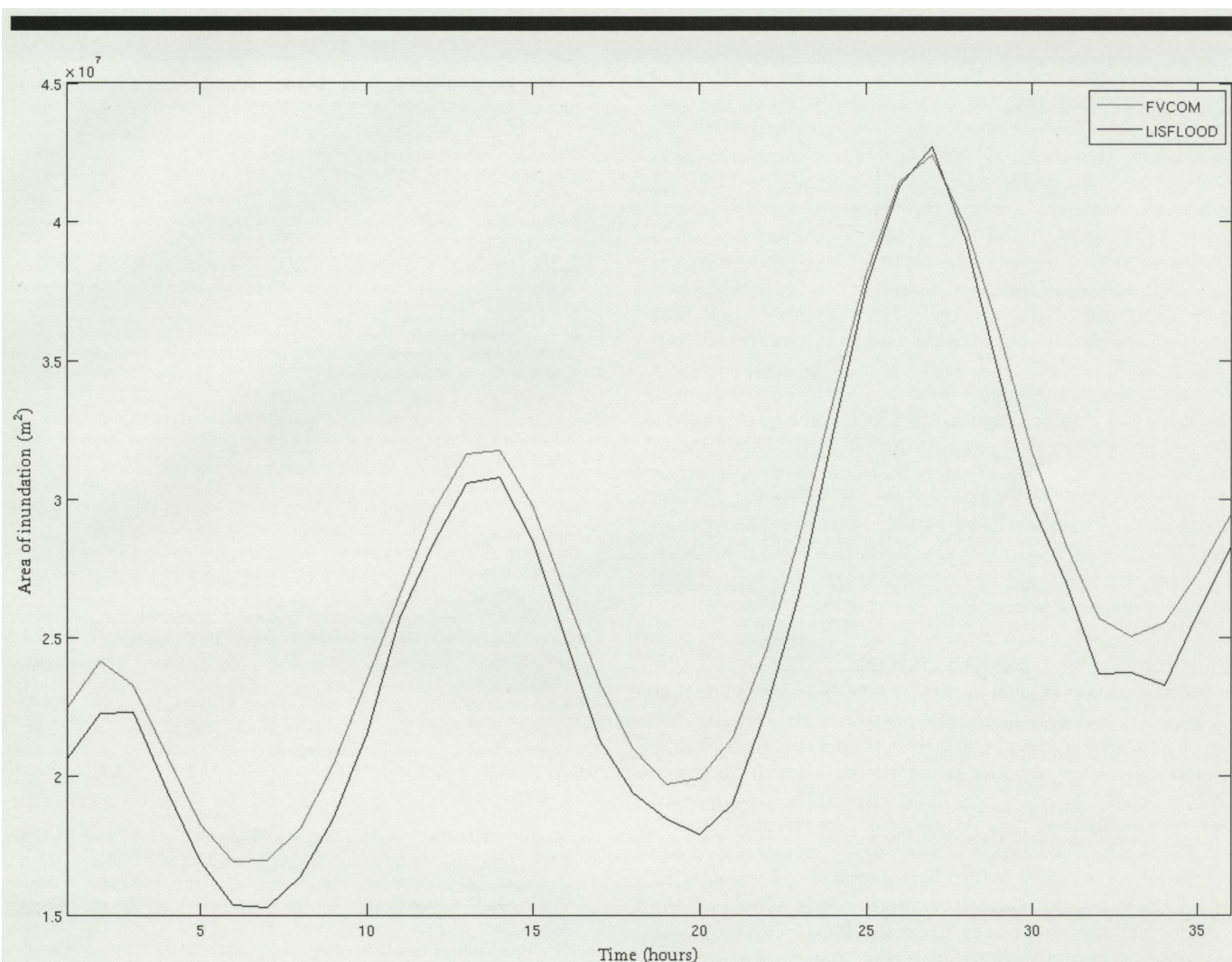


Figure 10. Time series of the area of inundation in IE4 due to a combined tide, surge (2 m), and river discharge ($600 \text{ m}^3 \text{ s}^{-1}$) in LISFLOOD-FP and FVCOM. (Color for this figure is available in the online version of this paper.)

which is equivalent to 28 cells on the LISFLOOD-FP model grid.

DISCUSSION

It was found that the combination of surge and river in idealised estuaries leads to interactions that increased residual elevations, particularly in IE1 where the tide and surge magnitude is still significant in the region of the river input. However, in the case of IE1, peak interactions occur in a region proximal to the river discharge at the closed boundary of the estuary, so any hydraulic damming or backwater effects cannot be accounted for. In the more elongate estuaries (IE2 and IE3) it was found that these interactions were insignificant, as the river input is more decoupled from the tide and surge input where the two components inundate the intertidal area without significant interaction in the mid-estuary. However, these idealised estuaries do not account for potential con-

straints of the river in the upper estuary due to natural topography or flood defences that could allow more interaction between the surge and river in the mid-estuary in a real estuary. In these idealised cases the river is allowed to flood and lose volume and momentum to the floodplain so that interactions in the mid-estuary are inhibited.

Interaction in IE1 was not found to cause any increases in the area of maximum inundation, which was found to be mainly determined by the surge magnitude. This was also observed in IE2 and IE3, where the maximum area of inundation decreased as the intertidal zone gradient increased. However, in a real estuary case with more variable topography and flood constraints, increases in elevation due to river-surge interaction in specific regions may have more implications for flooding if the increases are proximal to a flood defence or natural topographic feature that may be breached or overtopped. As these test cases are based on no-adaptation scenarios, construction of sea defences or river

defences could change the relative magnitude of the river discharge compared with the surge and alter the magnitude of the interactions within the estuary. Altering the timing of the peak river discharge did not significantly change the total area of inundation. In the case of the idealised estuaries tested here it was found that the area of inundation was controlled by the volumetric contribution of the tide and surge, which is dominant over any momentum exchange and interactions between the two components. Therefore, in a predictive sense for real estuaries the largest uncertainties may lie in the surge and river discharge boundary conditions that contribute to the estuary volume. It was found that although the simpler formulation used in the LISFLOOD-FP code generally simulated a lower area of inundation and a slightly less advanced flood front, the peak inundation was predicted to a similar extent as the FVCOM model that solves the full shallow-water equations. Although the computation of the code was different in both cases so that a direct comparison in the clock times could not be carried out, it was found that the LISFLOOD-FP model ran 24 times faster than the FVCOM model. However, it is likely that the LISFLOOD-FP model could be run much faster if the code was run in parallel over many processors.

CONCLUSION

On the basis of this study it can be assumed that operational inundation models of estuary regions can use approximations of the shallow-water equations that neglect inertial terms for simplicity and computational efficiency. Simpler model formulations allow ensembles to be carried out more easily to sample the range of uncertainty (Bates *et al.*, 2005). The flood extent is most likely dominated by the topography as opposed to the physics of the flood propagation and as long as the elevations in the mid-channel of the estuary are simulated accurately the flood extent may be simulated accurately where floodplain flow in the simpler model is of a realistic-enough nature (Horritt and Bates, 2001). As the surge is the dominant mechanism in inundation, future flood risk will mainly depend on the surge climate acting on increased sea levels where increases in mean sea level have been shown to have the largest effect on flood inundation. However, it must be noted that in real estuary cases surge-river interaction may be more significant, particularly if up-estuary flood defences or topographic constraints restrict inundation due to the river so that it interacts with the surge in the mid-estuary. Also, although in this instance it was assumed that the estuary was well mixed and that vertical stratification does not affect the inundation, this may not be true for all estuaries and should be included in cases where vertical stratification is significant and vertical mixing and gravitational circulation may affect the resultant inundation. The level of these interactions and its effect on any resultant inundation must be taken into account when planning operational inundation model schemes in real estuaries.

LITERATURE CITED

- Armi, L., 1986. The hydraulics of two flowing layers with different densities. *Journal of Fluid Mechanics*, 163(1), 27–58.
- Bates, P.D. and De Roo, A.P.J., 2000. A simple raster-based model for flood inundation simulation. *Journal of Hydrology*, 236(1), 54–77.
- Bates, P.D.; Dawson, R.J.; Hall, J.W.; Horritt, M.S.; Nicholls, R.J.; Wick, J., and Hassan, M.A.A.M., 2005. Simplified two-dimensional numerical modelling of coastal flooding and example applications. *Coastal Engineering*, 52(9), 793–810.
- Bates, P.D.; Horritt, M.S., and Fewtrell, T.J., 2010. A simple inertial formulation of the shallow water equations for efficient two-dimensional flood inundation modelling. *Journal of Hydrology*, 387(1), 33–45.
- Battjes, J.A. and Gerritsen, H., 2002. Coastal modelling for flood defence. *Philosophical Transactions of the Royal Society A*, 360(1796), 1461–1475.
- Chen, C.; Liu, H., and Beardsley, R.C., 2003. An unstructured grid, finite-volume, three-dimensional, primitive equations ocean model: application to coastal ocean and estuaries. *Journal of Atmospheric and Oceanic Technology*, 20(1), 159–186.
- Chen, S.N. and Sanford, L.P., 2009. Lateral circulation driven by boundary mixing and the associated transport of sediments in idealized partially mixed estuaries. *Continental Shelf Research*, 29(1), 101–118.
- Chen, S.N. and Sanford, L.P., 2009. Axial wind effects on stratification and longitudinal salt transport in an idealized, partially mixed estuary. *Journal of Physical Oceanography*, 39(8), 1905–1920.
- Flather, R.A., 2000. Existing operational oceanography. *Coastal Engineering*, 31(1), 13–40.
- Flowerdew, J.; Horsburgh, K.J.; Wilson, C., and Mylne, K., 2010. Development and evaluation of an ensemble forecasting system for coastal storm surges. *Quarterly Journal of the Royal Meteorological Society*, 136(651), 1444–1456.
- Horritt, M.S. and Bates, P.D., 2001. Predicting floodplain inundation: raster-based modelling versus the finite-element approach. *Hydrological Processes*, 15(5), 825–842.
- Horritt, M.S. and Bates, P.D., 2002. Evaluation of 1-D and 2-D numerical models for predicting river flood inundation. *Journal of Hydrology*, 268(1–4), 87–99.
- IPCC (International Panel on Climate Change), 2007. Climate change 2007: Impacts, adaptation, and Vulnerability. In: Parry, M.L.; Canziani, O.F.; Palutikof, J.P.; van der Linden, P.J., and Hanson, C.E. (eds.), *Contribution of Working Group II to the Fourth Assessment Report of the Intergovernmental Panel on Climate Change*. Cambridge, U.K.: Cambridge University Press, 976p.
- Jones, J.E. and Davies, A.M., 2005. An intercomparison between finite difference and finite element (TELEMAC) approaches to modelling west coast of Britain tides. *Ocean Dynamics*, 55(3–4), 178–198.
- Jones, J.E. and Davies, A.M., 2008. Storm surge computations for the west coast of Britain using a finite element model (TELEMAC). *Ocean Dynamics*, 58(5–6), 337–363.
- Lewis, M.; Bates, P.; Horsburgh, K.; Neal, J., and Schumann, G., 2012. Storm surge inundation model of the Northern Bay of Bengal using publicly available data. *Quarterly Journal of the Royal Meteorological Society*, 139(671), 358–369.
- Lewis, M.; Horsburgh, K.J.; Bates, P.D., and Smith, R., 2011. Quantifying the uncertainty in future coastal flood risk estimates for the U.K. *Journal of Coastal Research*, 27(5), 870–881.
- Lowe, J.A.; Howard, T.; Pardaens, A.; Tinker, J.; Holt, J.; Wakelin, S.; Milne, G.; Leake, J.; Wolf, J.; Horsburgh, K.; Reeder, T.; Jenkins, G.; Ridley, J.; Dye, S., and Bradley, S., 2009. *UK Climate Projections Science Report: Marine and Coastal Projections*. Exeter, U.K.: Met Office Hadley Centre.
- Lynch, D.R. and Gray, W.G., 1979. A wave equation model for finite element tidal computations. *Computer and Fluids*, 7(3), 207–228.
- Marks, K. And Bates, P.D., 2000. Integration of high-resolution topographic data with floodplain flow models. *Hydrological Processes*, 14(11–12), 2109–2122.
- McCowan, A.; Rasmussen, E., and Berg, P. 2001. Improving the performance of a two-dimensional hydraulic model for floodplain applications. Hobart, Australia: Conference on Hydraulics in Civil Engineering, 2001.

- Nicholls, Robert J., 2002 Analysis of global impacts of sea-level rise: a case study of flooding. *Physics and Chemistry of the Earth, Parts A/B/C*, 27, 1455–1466.
- Prestininzi, P.; Di Baldasarre, G.; Shumann, G.J.-P., and Bates, P.D., 2011. Selecting the appropriate hydraulic model structure using low-resolution satellite imagery. *Advances in Water Resources*, 34(1), 38–46.
- Robins, P., 2008. Present and future flooding scenarios in the Dyfi Estuary, Wales, U.K. *Report for the Countryside Council for Wales (number 3)* Bangor, U.K.: Centre for Applied Marine Sciences, Bangor University.
- Svensson, C. and Jones, D.A., 2004. Dependence between sea surge, river flow and precipitation in south and west Britain. *Hydrology and Earth System Sciences*, 8(5), 973–992.
- Westerlink, J.J.; Luettich, J.R., and Muccino, J.C., 1994. Modelling tides in the western North Atlantic using unstructured graded grids, *Tellus A*, 46(2), 178–199.
- Woodworth, P.L.; Teferle, N.; Bingley, R.; Shennan, I., and Williams, S.D.P., 2009. Trends in UK mean sea level revisited. *Geophysical Journal International*, 176(1), 19–30.